CrossMark

Comparison of ApoE-related brain connectivity differences in early MCI and normal aging populations: an fMRI study

Faye McKenna[1] · Bang-Bon Koo[2] · Ronald Killiany[2,3] · for the Alzheimer's Disease Neuroimaging Initiative

Abstract In this study, we used resting-state functional magnetic resonance imaging (rs-fMRI) scans from subjects with early mild cognitive impairment (EMCI) and control subjects to study functional network connectivity. The scans were acquired by the Alzheimer's Disease Neuroimaging Initiative (ADNI). We used genetic data from the ADNI database to further subdivide the EMCI and control groups into genotype groups with or without the Apolipoprotein E allele e4 (APOE e4). Region of interest (ROI)-to-ROI resting-state functional connectivity was measured using Freesurfer and the Functional Connectivity Toolbox for Matlab (CONN). In our analysis, we compared whole-brain ROI connectivity strength and ROI-to-ROI functional network connectivity strength between EMCI, control and genotype subject groups. We found that the ROI network properties were disrupted in EMCI and APOE e4 carrier groups. Notably, we show that (1) EMCI disrupts functional connectivity strength in many important functionally-linked areas; (2) APOE e4 disrupts functional connectivity strength in similar areas to EMCI; and (3) the differences in functional connectivity between groups shows a multifactor contribution to functional network dysfunction along the trajectory leading to dementia.

Keywords EMCI · Dementia · RS-fMRI · APOE e4

✉ Faye McKenna
  faye.mckenna@ucsf.edu

[1] Bioimaging Program, Boston University School of Medicine, 650 Albany Street, Boston, MA 02118, USA

[2] Department of Anatomy and Neurobiology, Boston University School of Medicine, 72 East Concord Street, Boston, MA 02118, USA

[3] Center for Biomedical Imaging Boston University School of Medicine, 650 Albany Street, Boston, MA 02118, USA

Introduction

Alzheimer's disease (AD) is one of the most common neurodegenerative diseases in the world, and is clinically characterized by memory and cognitive impairments (Petersen et al. 1999). Early mild cognitive impairment (EMCI) is thought of as the mildest symptomatic phase on the trajectory leading to AD, and the transitional state between normal aging and AD (Mueller et al. 2005). Investigating EMCI is particularly important because 27 % of those with EMCI have been recorded to convert to AD (Jessen et al. 2014). It is hypothesized that Alzheimer's disease pathology is multifactorial, and a major focus of EMCI and AD research has been to try to determine the diseases' contributing factors (Mueller et al. 2005). There are several distinct factors known to contribute to AD, one of the most significant is the Apolipoprotein E allele e4 (APOE e4) (Buckner 2004). The APOE allele e4 is the best-established genetic risk factor for sporadic AD, and it increases the life-time risk of developing AD 3 to 15 times (Mahley et al. 2006). Previous research has shown that APOE e4 modulates brain activity of both normal and AD patients as measured by fMRI (Machulda et al. 2011).

In the current study we sampled resting-state fMRI scans of EMCI patients with matched controls from the ADNI database (http://adni.loni.usc.edu/data-samples/access-data/) to

investigate the hypothesis that EMCI is characterized by disruptions of functional connectivity in brain networks associated with memory and cognitive functioning. We also evaluated the effects of APOE e4 on functional network connectivity by comparing ROI network connections in all subjects with and without APOE e4. In doing this, we examined how this genetic predisposition contributes to brain dysfunction, and how it compares to the pathology observed in the EMCI phenotype.

Most information about how AD and its earlier stages affect brain morphometry come from post-mortem ex-vivo analysis and structural MRI (Buckner 2004). Resting state-fMRI (rs-fMRI) is a popular and reliable tool for studying functional connectivity, which has been successfully used to investigate aging and dementia (Sanz-Arigita et al. 2010; Sheline et al. 2010; Wang et al. 2007). Abnormal functional connectivity patterns have been found to be a potential biomarker for the diagnosis of AD and EMCI (Greicius et al. 2004; Wang et al. 2007). A primary method used to investigate the functional connectivity of specific brain regions is by seed-driven resting state functional connectivity (RSFC) analysis (Fox et al. 2005). In this study we use the NITRC Functional Connectivity Toolbox (CONN) for Matlab, created by MIT to implement the seed-driven ROI-to-ROI RSFC analysis strategy (Whitfield-Gabrieli and Nieto-Castanon 2012).

The neural basis underlying the functional damage in EMCI is not yet fully understood. Previous fMRI studies have revealed that the cognitive function deficits in Alzheimer's disease and its earlier stages could be due to abnormalities in the connectivity between brain areas (Supekar et al. 2008). Recently, multimodal imaging studies have provided evidence that Alzheimer's disease is a disconnection syndrome, but there is not a convergence on the network pattern (Delbeuck et al. 2007). The disconnection syndrome interpretation of dementia pathology is exciting because it could account for dementia's complex symptomatology (Delbeuck et al. 2007). It is less probable that dementia is a result of pathophysiology in one neuronal system, but instead a consequence of an alteration in the brain's connectivity between several neuronal systems (Delbeuck et al. 2007). Through rs-fMRI connectivity analysis, this study examined the evidence that points to Alzheimer's disease, in its earlier form of EMCI, as being a disconnection syndrome. The focus of this study was also to investigate how APOE e4 contributes to RSFC dysfunction. To our knowledge, no other study has investigated resting-state fMRI data of an EMCI population with APOE data. This research is particularly important because it investigates the multi-dimensional component of dementia pathology. We hypothesized that (1) There is significant disruption of RSFC in EMCI (2) APOE e4 carriers show unique and significant disruption in RSFC.

Materials and methods

Overview of ADNI

All data used in the preparation of this article were obtained from the Alzheimer's Disease Neuroimaging Initiative (ADNI) database (www.loni.ucla.edu/ADNI). The ADNI was launched in 2003 by the National Institute on Aging, the National Institute of Biomedical Imaging and Bioengineering, the Food and Drug Administration, private pharmaceutical companies and non-profit organizations, as a $60 million, 5-year public-private partnership. The primary goal of ADNI has been to test whether serial MRI, positron emission tomography, other biological markers, and clinical and neuropsychological assessment can be combined to measure the progression of MCI and early AD. Determination of sensitive and specific markers of very early AD progression is intended to aid researchers and clinicians to develop new treatments and monitor their effectiveness, as well as lessen the time and cost of clinical trials. The Principal Investigator of this initiative is Michael W. Weiner, MD, VA Medical Center and University of California – San Francisco. ADNI is the result of efforts of many co-investigators from a broad range of academic institutions and private corporations, and subjects have been recruited from over 50 sites across the U. S. and Canada. The initial goal of ADNI was to recruit 800 subjects but ADNI has been followed by ADNI-GO and ADNI-2. To date these three protocols have recruited over 1500 adults, ages 55 to 90, to participate in the research, consisting of cognitively normal older individuals, people with early or late MCI, and people with early AD. The follow up duration of each group is specified in the protocols for ADNI-1, ADNI-2 and ADNI-GO. Subjects originally recruited for ADNI-1 and ADNI-GO had the option to be followed in ADNI-2. For up-to-date information, see www.adni-info.org.

Subjects

The ADNI data was screened for subjects who were either EMCI or control, had base-line resting-state fMRI scans, and were in the ADNI2 or ADNIGO phases at the time this study started. ADNIGO and ADNI2 are the two latest stages in the ADNI study and include the EMCI subject grouping. Out of the initial 44-screened subjects 4 were omitted due to anatomical abnormalities in their MRI scans, and 4 were omitted because of missing information. This left 36 subjects selected from the database ($N=36$),18 EMCI and 18 matched control subjects. Out of the 36 subjects 9 were taken from ADNIGO and 27 were taken from ADNI2.

Control and EMCI subjects were matched based on age, sex, education and Multi-Mini State Examination (MMSE) score (See Table 1). R-Studio was used to run t-tests and ensure that there was no difference in age, sex, education, MMSE and genotype between the groups (see Table 1) (RStudio 2014).

Table 1 EMCI/control matching statistics

Variable	t	df	p-value
APOE	0.8092	33.912	0.424
MMSE Score	−0.2667	31.523	0.7914
Education	−0.2542	33.998	0.8008
Age	−0.0615	31.354	0.9514
Sex	0.3523	33.911	0.7268

T-tests were run to show there are no significant differences in genotype, MMSE score, education, age or sex between the EMCI and control subject groups

The mean age was 69.72±13.21, mean MMSE score 28.72± 1.23 and mean education 15.78±2.59 (see Table 2). Out of the subjects 10 were men and 26 were women, equally distributed as EMCI and Control subjects (see Table 2). There were 14 subjects that were APOE e4 carriers: 6 control and 8 EMCI (See Table 2). There were 22 subjects that were APOE e4 non-carriers: 12 control and 10 EMCI (see Table 2). The *APOE* subject groups had no significant difference in age, sex, MMSE score, and education (see Tables 1 and 2).

Neuropsychological measures

All subjects in the ADNI program complete a battery of neuropsychological tests and demographic information to screen for existing pathologies and dementia diagnosis (Petersen and Weiner 2014). The ADNI uses the following tests and scales for screening: Clinical Dementia Rating Memory, Clinical Dementia Rating problem solving and judgment, Mini Mental State Examination, Montreal Cognitive Assessment, Everyday Cognition, Clock Drawing Test, Activities of Daily Living FAQ, Neuropsychiatric Inventory, Geriatric Depression Scale,

Concomitant Medications, Vital Signs, and Diagnostic Summary (Petersen and Weiner 2014). Based on cognitive tests, the subjects were classified by the ADNI clinical score as: (a) normal controls with normal cognition and memory, Mini Mental Status Exam (MMSE) between 24 and 30, Clinical Dementia Rating (CDR) 0; (b) EMCI with a memory complaint verified by a study partner, abnormal memory function documented by scoring below the education adjusted cutoff on the Logical Memory II subscale from the Wechsler Memory Scale-Revised (Roid et al. 2007), MMSE score between 24 and 30, CDR 0.5, memory box score at least 0.5, absence of dementia observed by physician at time of screening visit, preserved activities of daily living; (c) Amnestic Mild Cognitive Impairment with memory complaint verified by a study partner, memory loss measured by education-adjusted performance on the Logical Memory II subscale of the Wechsler Memory Scale-Revised (Roid et al. 2007), memory box score at least 0.5, MMSE between 24 and 30, CDR 0.5, absence of dementia observed by physician at time of screening visit, preserved activities of daily living; (d) probable AD with memory complaint validated by study partner, abnormal memory function for age and education level, impaired activities of daily living, reduced cognition, CDR>0.5, MMSE between 20 and 26 (Petersen and Weiner 2014). For this study only control and EMCI data was used.

Genetic testing

Whole blood samples were collected at baseline for all subjects for APOE genotyping by the ADNI and processed at the National Cell Repository for AD (NCRAD) for genotyping (Peterson and Weiner 2014). For ADNI2 and ADNIGO genotyping was performed using the Illumina Human Omni Express Bead Chip, which contains 730,525 SNP markers, according to the manufacturer's protocols (Petersen and

Table 2 ADNI sample demographics

Measures	All	Controls	EMCI	APOE e4 +	APOE e4 -
N	36	18	18	14	22
Mean Age (yrs)	69.72	67.61	71.83	70.21	72.77
SD Age (yrs)	13.21	17.55	6.47	3.79	6.4
Median Age (yrs)	71.2	71.35	71.45	70.8	72.5
Mean MMSE score	28.72	28.67	28.78	28.79	28.68
SD MMSE score	1.23	1.41	1.06	1.37	1.17
Median MMSE score	29	29	29	29	29
Mean Ed (yrs)	15.78	15.67	15.89	15.85	15.6
SD Ed (yrs)	2.59	2.61	2.63	2.61	2.53
Median Ed (yrs)	16	16	16	16	16
Male	10	5	5	4	6
Female	26	13	13	8	18
APOE e4 carrier	14	6	8	–	–
APOE e4 non-carrier	22	12	10	–	–

Shows all statistics for EMCI/Control groups and APOE e4 carrier and APOE e4 non-carrier groups

Weiner 2014). For this study we grouped the subjects into two groups, with and without the APOE allele e4.

Imaging

Imaging acquisition

All subjects were scanned on 3.0 Tesla Philips MRI scanners, either an Intera or Achieva model at a participating ADNI research site. The ADNI MRI protocol obtained an array of images for each subject, and for this study we used the structural MRI and resting-state fMRI scans. The structural MRI MPRAGE scans were obtained with T1-weighting; 1.2 slice thickness, and sagittal acquisition plane. The T2* fMRI resting-state scans were obtained using an echo-planar imaging sequence with the following parameters: 140 time points; repetition time (TR)=3000 ms; echo time (TE)=30 ms; flip angle=80°, number of slices=48; slice thickness=3.3 mm spatial resolution=$3 \times 3 \times 3$ mm3 and matrix=64×64 (Petersen and Weiner 2014). EPI is a fast magnetic resonance imaging technique that allows acquisition of single images in as little as 20 msec and performance of multiple-image studies in as little as 20 s (DeLaPaz 1994). All original image files are available to the general scientific community.

Resting-state functional connectivity pre-processing

All of the subject's original MPRAGE scans in DICOM format were downloaded from the ADNI database and processed using FreeSurfer version 5.3. FreeSurfer (FreeSurfer.net) is a software application developed by the Martinos Center for Biomedical Imaging by the Laboratory for Computational Neuroimaging (*FreeSurfer Wiki*, 2014). The FreeSurfer recon-all pipeline was used for: motion correction, intensity normalization, talairach transformation, skull stripping, segmentation of the cortex, subcortex and white matter, to generate surfaces and create spherical and flattened representations. In this study we used the Desikan-Killiany atlas script for cortical segmentation. Freesurfer's Freeview was used to inspect the recon-all processing output. Some white matter and gray matter subcortical segmentation defects that were fixed manually, and the corresponding processing step in the recon-all pipeline were re-run for correction.

Resting-state functional connectivity processing

The CONN toolbox was used for RSFC analysis. CONN is a Matlab-based cross-platform software that was used to compute and analyze the functional connectivity of fMRI (Whitfield-Gabrieli and Nieto-Castanon 2012). The CONN toolbox utilized Matlab version 2012 and SPM8 to process the resting-state fMRI scans into ROI-to-ROI connectivity matrices, test hypotheses and visualize data (Whitfield-

Gabrieli and Nieto-Castanon 2012). CONN used the CompCor strategy for spatial and temporal preprocessing to define and remove confounds in the blood-oxygen-level dependent (BOLD) signal to prevent the impact of physiological noise factors and motion in the data (Behzadi et al. 2007). CONN used a seed-driven RSFC analysis strategy, where the Pearson's correlation coefficient was calculated between the seed time course and the time course of all other voxels (Whitfield-Gabrieli and Nieto-Castanon 2012). After, the correlation coefficients were converted to normally distributed scores using Fisher's transformation to allow for second-level General Linear Model analysis (Whitfield-Gabrieli and Nieto-Castanon 2012). The correlation maps were dependent on the specific location of the seed so that functionally and anatomically heterogeneous ROI were dissociated in order to delineate functional anatomy in the brain by sharp transitions in correlation patterns that signal functional boundaries across the cortex (Whitfield-Gabrieli and Nieto-Castanon 2012). CONN created subject-specific ROI files for 105 ROIs and registered them to the subject space, which included four FOX ROIs and all the Brodmann areas (see Table 3). These ROI were used as the seeds of interest for whole-brain subject-specific ROI-ROI connectivity analyses.

Statistical analysis

Functional connectivity measures were computed between seed areas for ROI-to-ROI analysis and to create ROI-to-ROI connectivity. The CONN toolbox used a linear measure of functional connectivity between bivariate correlation and bivariate-regression coefficients, with their associated multivariate measures of semipartial-correlation and multivariate-regression coefficients to calculate functional connectivity (Whitfield-Gabrieli and Nieto-Castanon 2012). After each subject had ROI-to-ROI connectivity matrices the ROI-level analyses were evaluated through F- or Wilks lambda statistics depending on the dimensionality of the within and between subjects contrasts. Connectivity contrast effect size between all ROI sources was calculated alongside T,F,X values, uncorrected p-values and FDR-corrected p-values for each specified second-level analysis. The F-test was used to calculate the multivariate connectivity strength for each seed and seed/network-level thresholds.

We tested: the EMCI versus control subject group interaction, the APOE e4 carrier versus non-carrier group interaction, and the control APOE e4 non-carrier group versus the other groups interaction. The significance of ROI-to-ROI connection was determined through the false positive control false discovery rate (FDR)-corrected *p*-values with a chi-squared test with two-sided inferences. This false-positive control test was implemented through both a voxel-level height threshold and a cluster-level extent threshold defined by the uncorrected *p*-values. The EMCI versus control group connectivity analysis was thresholded at .00001 FDR- corrected p-values for

Table 3 ROI list

Region	
BA.1 (L). Primary Somatosensory Cortex	BA.35 (L). Perirhinal cortex
BA.1 (R). Primary Somatosensory Cortex	BA.35 (R). Perirhinal cortex
BA.10 (L). Anterior Prefrontal Cortex	BA.36 (L). Parahippocampal cortex
BA.10 (R). Anterior Prefrontal Cortex	BA.36 (R). Parahippocampal cortex
BA.11 (L). Orbitofrontal Cortex	BA.37 (L). Fusiform gyrus
BA.11 (R). Orbitofrontal Cortex	BA.37 (R). Fusiform gyrus
BA.13 (L). Insular Cortex	BA.38 (L). Temporopolar Area
BA.13 (R). Insular Cortex	BA.38 (R). Temporopolar Area
BA.17 (L). Primary Visual Cortex	BA.39 (L). Angular gyrus
BA.17 (R). Primary Visual Cortex	BA.39 (R). Angular gyrus
BA.18 (L). Secondary Visual Cortex	BA.4 (L). Primary Motor Cortex
BA.18 (R). Secondary Visual Cortex	BA.4 (R). Primary Motor Cortex
BA.19 (L). Associative Visual Cortex	BA.40 (L). Supramarginal Gyrus
BA.19 (R). Associative Visual Cortex	BA.40 (R). Supramarginal Gyrus
BA.2 (L). Primary Somatosensory Cortex	BA.41 (L). Primary Auditory Cortex
BA.2 (R). Primary Somatosensory Cortex	BA.41 (R). Primary Auditory Cortex
BA.20 (L). Inferior Temporal Gyrus	BA.42 (L). Primary Auditory Cortex
BA.20 (R). Inferior Temporal Gyrus	BA.42 (R). Primary Auditory Cortex
BA.21 (L). Middle Temporal Gyrus	BA.43 (L). Subcentral Area
BA.21 (R). Middle Temporal Gyrus	BA.43 (R). Subcentral Area
BA.22 (L). Superior Temporal Gyrus	BA.44 (L). IFC pars opercularis
BA.22 (R). Superior Temporal Gyrus	BA.44 (R). IFC pars opercularis
BA.23 (L). Ventral Posterior Cingulate Cortex	BA.45 (L). IFC pars triangularis
BA.23 (R). Ventral Posterior Cingulate Cortex	BA.45 (R). IFC pars triangularis
BA.24 (L). Ventral Anterior Cingulate Cortex	BA.46 (L). Dorsolateral Prefrontal Cortex
BA.24 (R). Ventral Anterior Cingulate Cortex	BA.46 (R). Dorsolateral Prefrontal Cortex
BA.25 (L). Subgenual cortex	BA.47 (L). Inferior Prefrontal Gyrus
BA.25 (R). Subgenual cortex	BA.47 (R). Inferior Prefrontal Gyrus
BA.27 (L). Piriform Cortex	BA.5 (L). Somatosensory Association Cortex
BA.27 (R). Piriform Cortex	BA.5 (R). Somatosensory Association Cortex
BA.28 (L). Posterior Entorhinal Cortex	BA.6 (L). Premotor Cortex
BA.28 (R). Posterior Entorhinal Cortex	BA.6 (R). Premotor Cortex
BA.29 (L). Retrosplenial Cingulate Cortex	BA.7 (L). Somatosensory Association Cortex
BA.29 (R). Retrosplenial Cingulate Cortex	BA.7 (R). Somatosensory Association Cortex
BA.3 (L). Primary Somatosensory Cortex	BA.8 (L). Dorsal Frontal Cortex
BA.3 (R). Primary Somatosensory Cortex	BA.8 (R). Dorsal Frontal Cortex
BA.30 (L). Cingulate Cortex	BA.9 (L). Dorsolateral Prefrontal Cortex
BA.30 (R). Cingulate Cortex	BA.9 (R). Dorsolateral Prefrontal Cortex
BA.31 (L). Dorsal Posterior Cingulate Cortex	Precuneus (PCC) (0,−56,28)
BA.31 (R). Dorsal Posterior Cingulate Cortex	Right Inferior Parietal Lobe (RLP) (48,−60,38)
BA.32 (L). Dorsal anterior Cingulate Cortex	Left Inferior Parietal Lobe (LLP) (−42,−68,38)
BA.32 (R). Dorsal anterior Cingulate Cortex	Med Prefrontal Cortex (MPFC) (0,54,−8)
BA.33 (L). Anterior Cingulate Cortex	Right Posterior Sup Temp Gyrus (60,−30,24)
BA.33 (R). Anterior Cingulate Cortex	Right Anterior Sup Temp Gyrus (54,8,−2)
BA.34 (L). Anterior Entorhinal Cortex	Cingulate Gyrus (0,6,40)
BA.34 (R). Anterior Entorhinal Cortex	Right Superior Frontal Gyrus (30,22,52)
	Left Superior Frontal Gyrus (−28,22,52)
	Left Posterior Sup Temp Gyrus (−60,−30,20)
	Left Anterior Sup Temp Gyrus (−44,4,−4)

105 ROI (47 in each hemisphere), more details about cerebral parcellation can be found in (Whitfield-Gabrieli and Nieto-Castanon 2012)

both the voxel-level height threshold and cluster-level extent threshold ROI-ROI and seed ROI tests. The APOE e4 carrier versus non-carrier group connectivity analysis was thresholded at .00001 FDR- corrected p-values for both the voxel-level height threshold and cluster-level extent threshold for ROI-ROI and seed ROI tests. The APOE e4 non-carrier group versus other subject groups' connectivity analysis was thresholded at .00001 FDR- corrected p-values for both the voxel-level height threshold and cluster-level extent threshold for ROI-ROI and seed ROI tests. The CONN toolbox seed-to-voxel and ROI-to-ROI analyses results are considered appropriately corrected for multiple comparisons across all brain and analysis voxels when the height voxel-level and the extent cluster-level thresholds use an analysis-wise false positive control FDR-corrected p-values method (Whitfield-Gabrieli and Nieto-Castanon 2012).

Results

Subject group differences

We found significant differences in brain connectivity between the EMCI and control subjects. Control individuals had significantly stronger network connections notably in 10 ROI at the .00001 FDR-p value thresholded for both seed and network levels (see Table 4, Fig. 1). Control individuals had 16 significantly stronger ROI-ROI specific connections (see Table 5). No ROI or ROI-ROI connection strength was more significant in EMCI than in control subjects at a significant threshold. The 'intensity' and 'size' measures represent alternative ways to jointly evaluate whether the connectivity between the chosen seed ROI and all other ROIs shows any significant effect of interest (Whitfield-Gabrieli and Nieto-Castanon 2012). These measures represent the number of suprathrehsold connections between this seed and all other

ROIs above the threshold, and their overall strength as the sum of absolute T-values over these suprathreshold conections (Whitfield-Gabrieli and Nieto-Castanon 2012).

APOE group differences

We found significant differences in brain connectivity between subjects with variance in APOE expression. Those who did not have a copy of the APOE allele e4, had stronger ROI connectivity in 7 ROI (see Table 6, Fig. 2). This group also had 29 significantly stronger ROI-ROI specific connections (see Table 7). The group that did have a copy of the APOE allele e4 had no ROI or ROI-ROI connection strength that was more significant than the group without APOE e4 at any significant threshold. The 'intensity' and 'size' measures represent the number of suprathrehsold connections between this seed and all other ROIs above the threshold, and their overall strength as the sum of absolute T-values over these suprathreshold conections (Whitfield-Gabrieli and Nieto-Castanon 2012).

APOE group versus subject group

We found significant differences in brain connectivity in subjects with or without APOE allele E4 and in different subject groups. Subjects who did not have APOE e4 and were also controls, had stronger ROI connectivity in 3 ROI (see Table 8, Fig. 3). The same group had 21 significantly stronger ROI-ROI specific connections (see Table 9). The subjects who either had APOE e4 and/or were EMCI had No ROI or ROI-ROI connection strengths that were significant at the .00001 significant threshold. The 'intensity' and 'size' measures represent the number of suprathrehsold connections between this seed and all other ROIs above the threshold, and their overall strength as the sum of absolute T-values over these suprathreshold conections (Whitfield-Gabrieli and Nieto-Castanon 2012).

Table 4   Group-normal versus EMCI

ROI	Area	Stats	Intensity	Size	P-FDR value	P-Unc value
17L	Left primary visual cortex	X(16)=70.22	560.66	6	0.0000	0.0000
18R	Right Inferior temporal gyrus	X(16)=69.76	585.80	11	0.0000	0.0000
85	Precuneus	X(16)=66.46	491.91	10	0.0000	0.0000
18L	Left secondary visual cortex	X(16)=65.78	695.07	11	0.0000	0.0000
19L	Left Associative visual cortex	X(16)=65.18	680.48	18	0.0000	0.0000
29R	Right retrosplenial cingulate cortex	X(16)=62.56	378.51	6	0.0000	0.0000
17R	Right primary visual cortex	X(16)=62.33	465.49	8	0.0000	0.0000
31L	Left dorsal posterior cingulate cortex	X(16)=59.49	446.99	12	0.0000	0.0000
19R	Right associative visual cortex	X(16) =59.47	508.00	12	0.0000	0.0000
32R	Left dorsal anterior cingulate cortex	X(16) =59.11	254.61	9	0.0000	0.0000

The More Significantly Connected Regions In Control Versus EMCI Subjects. In this table we only included ROI that were more significantly connected at a .00001 two-sided FDR-p value

Fig. 1 Superior, inferior, right, left, posterior view control > EMCI connectivity: shows significant ROI, and ROI-ROI connection in control versus EMCI subject group. *Red* to *green*=more to less significant
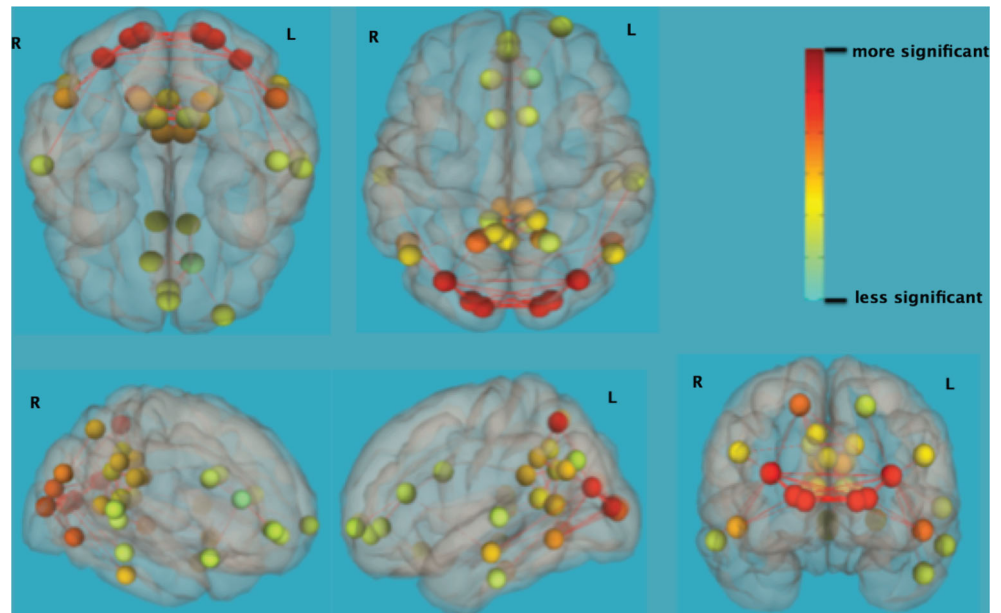
Discussion

Comparison of EMCI versus control subject group network connectivity differences

We found significant differences in the functional architecture of the healthy aging brain and the EMCI brain at rest. The EMCI group showed decreased RSFC strength in ROIs and decreased activation of ROI-to-ROI connections at the .00001 FDR-p threshold level (see Tables 3 and 4). These decreases in

ROI connectivity strength reflect the decrease in activity coherence of the ROI (Whitfield-Gabrieli and Nieto-Castanon 2012).

Pre-frontal lobe

The most notable difference between the EMCI group RSFC decrease and the APOE e4 carrier group RSFC decrease was in frontal lobe structures. As discussed previously, both EMCI and APOE e4 carrier groups are known to have a high

Table 5 Group- normal versus EMCI connections

ROI	Area	Strength	P-unc value	P-FDR value
17L-18L	L Primary Visual Cortex- L Secondary Visual Cortex	F(2)(34)=186.91	0.0000	0.0000
18L-19L	L Secondary Visual Cortex- L Associative Visual Cortex	F(2)(34)=139.21	0.0000	0.0000
29R-28L	R Retrosplenial Cingulate Cortex- L Posterior Entorhinal Cortex	F(2)(34)=138.84	0.0000	0.0000
17R-18R	R Primary Visual Cortex- R Secondary Visual Cortex	F(2)(34)=113.24	0.0000	0.0000
18R-18L	R &L Secondary Visual Cortex	F(2)(34)=108.70	0.0000	0.0000
17R-17L	R & L Primary Visual Cortex	F(2)(34)=103.37	0.0000	0.0000
17L-18R	L Primary Visual Cortex- R Secondary Visual Cortex	F(2)(34)=100.74	0.0000	0.0000
17L-19L	L Primary Visual Cortex- L Associative Visual Cortex	F(2)(34)=90.96	0.0000	0.0000
31L-31R	R&L Dorsal Posterior Cingulate Cortex	F(2)(34)=77.83	0.0000	0.0000
19R-18R	R Associative Visual Cortex- R Secondary Visual Cortex	F(2)(34)=76.41	0.0000	0.0000
(85)-PCC	Precuneus- Posterior Cingulate Cortex	F(2)(34)=71.72	0.0000	0.0000
17R-19R	R Primary Visual Cortex- R Associative Visual Cortex	F(2)(34)=69.78	0.0000	0.0000
31L-PCC	L Dorsal Posterior Cingulate Cortex-Posterior Cingulate Cortex	F(2)(34)=68.01	0.0000	0.0000
18L-17R	L Secondary Visual Cortex -R Primary Visual Cortex	F(2)(34)=64.55	0.0000	0.0000
29R-(85)	R Retrosplenial Cingulate Cortex- Precuneus	F(2)(34)=64.39	0.0000	0.0000
29R-30L	R Retrosplenial Cingulate Cortex-L Cingulate Cortex	F(2)(34)=64.25	0.0000	0.0000

The More Significant ROI-ROI Connections In Control Versus EMCI Subjects. In this table we only included ROI-ROI connections that were more significantly connected at a .00001 two-sided FDR-p value

Table 6 *APOE* group ROI

ROI	Area	Stats	Intensity	Size	P-unc value	P-FDR value
85	Precuneus	F(8)(28)=13.93	81.90	10	0.0000	0.0000
17L	(L). Primary Visual Cortex	F(8)(28)=13.37	62.39	7	0.0000	0.0000
29R	(R) Retrosplenial Cingulate Cortex	F(8)(28)=12.99	54.51	6	0.0000	0.0000
29L	(L) Retrosplenial Cingulate Cortex	F(8)(28)=12.51	45.54	5	0.0000	0.0000
18R	(R) Secondary Visual Cortex	F(8)(28)=12.32	86.47	11	0.0000	0.0000
18L	(L) Secondary Visual Cortex	F(8)(28)=11.86	88.28	11	0.0000	0.0000
17R	(R) Primary Visual Cortex	F(8)(28)=11.27	81.99	11	0.0000	0.0000

The More Significantly Connected Regions APOE e4 Carriers Versus Non-Carriers. In this table we only included ROI that were more significantly connected at a .00001 two-sided FDR-p value

susceptibility for developing AD. Uniquely, the EMCI group showed significant decrease in ROI strength and connectivity in the left dorsal anterior cingulate cortex and its connections with the medial prefrontal cortex (MPFC), anterior prefrontal cortex, right dorsal anterior cingulate cortex, and right and left ventral anterior cingulate cortices (see Fig. 1). This finding suggests that EMCI has some pathology unassociated with the APOE e4 pathology, which strongly affects areas in the prefrontal cortex. The prefrontal cortex has been shown to atrophy naturally with old age (Euston et al. 2002a, b). Since the EMCI and control groups were age-matched, our findings illustrate how EMCI pathology significantly affects the RSFC of the prefrontal lobe regardless of other age-related morphometric changes. This finding further strengthens the idea that AD pathology has multiple factors, and suggests that the weakness in frontal lobe connectivity seen in the EMCI subjects is mostly due to factors other than the APOE e4.

Surrounding hippocampal areas

The surrounding hippocampal areas in the medial temporal lobe (MTL) are known to be affected by AD pathology and show atrophy in structural analysis. This is consistent with our findings of decreased functional activity in the medial temporal gyrus, precuneus, dorsal posterior cingulate cortex, dorsal anterior cingulate cortex, and right retrosplenial cingulate cortex of EMCI subjects (see Fig. 1) (Buckner 2004). The hippocampus is regarded as the memory center, but it is closely linked both functionally and physically to these other anatomy with important executive functions (Buckner 2004). For example, the retrosplenial cortex acts as an interface zone between working memory functions enabled by the prefrontal cortex and long-term memory functions of the medial temporal lobe memory system (Kobayashi and Amaral 2003). Therefore, its decrease in function observed in the EMCI subjects could cause widespread and significant memory

Fig. 2 Superior, inferior, right, left, anterior view APOE e4 non-carriers > APOE e4 carriers connectivity: shows the more significant ROI, and ROI-ROI connections in the without APOE e4 group versus with APOE e4 group. *Red* to *green*=more to less significant
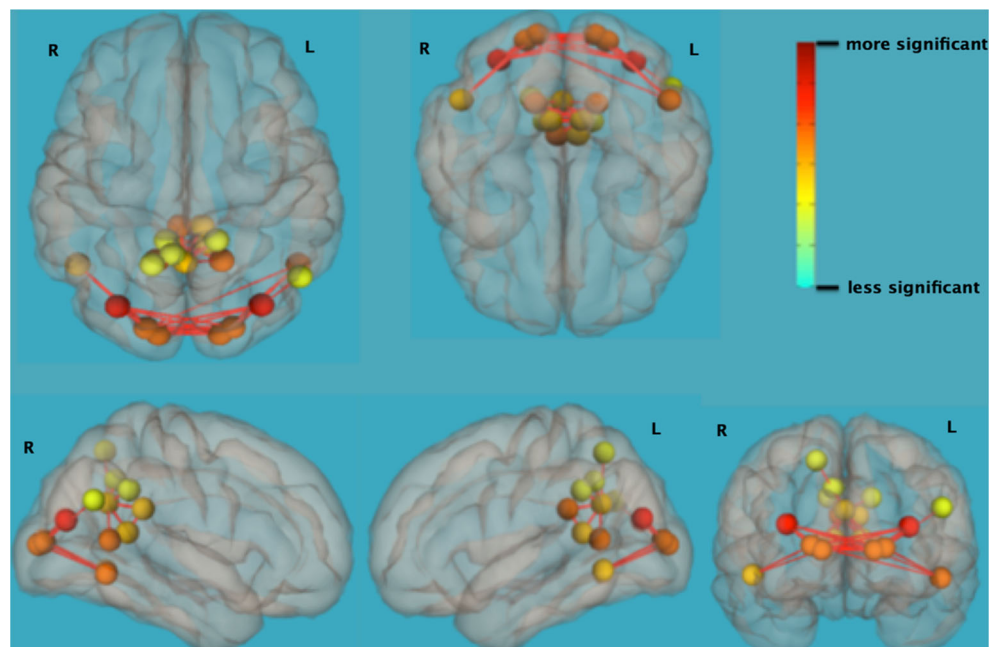
Table 7 *APOE* group connections

ROI	Area	Strength	P-unc value	P-FDR value
29R-29L	(R). Retrosplenial Cingulate Cortex -(L). Retrosplenial Cingulate Cortex	T(35)=12.38	0.0000	0.0000
18L-17L	(L). Secondary Visual Cortex-(L). Primary Visual Cortex	T(35)=12.05	0.0000	0.0000
18L-19L	(L). Secondary Visual Cortex-(L). Associative Visual Cortex	T(35)=11.64	0.0000	0.0000
17R-18R	(R). Primary Visual Cortex- (R). Secondary Visual Cortex	T(35)=10.80	0.0000	0.0000
19R-18R	(R). Associative Visual Cortex -(R). Secondary Visual Cortex	T(35)=10.53	0.0000	0.0000
17R-19R	(R). Primary Visual Cortex-(R). Associative Visual Cortex	T(35)=10.24	0.0000	0.0000
18R-18L	(R). Secondary Visual Cortex-(L). Secondary Visual Cortex	T(35)=10.18	0.0000	0.0000
17L-19L	(L). Primary Visual Cortex-(L). Associative Visual Cortex	T(35)=10.07	0.0000	0.0000
17L-17R	(L). Primary Visual Cortex- R). Primary Visual Cortex	T(35)=10.06	0.0000	0.0000
18R-17L	(R). Secondary Visual Cortex -(L). Primary Visual Cortex	T(35)=9.88	0.0000	0.0000
29L-30L	(L). Retrosplenial Cingulate Cortex -(L). Cingulate Cortex	T(35)=9.74	0.0000	0.0000
30L-29R	(L). Cingulate Cortex-(R). Retrosplenial Cingulate Cortex	T(35)=9.60	0.0000	0.0000
23L-85	(L). Ventral Posterior Cingulate Cortex- Precuneus	T(35)=9.44	0.0000	0.0000
85-23R	Precuneus-(R). Ventral Posterior Cingulate Cortex	T(35)=9.07	0.0000	0.0000
29R-23L	(R). Retrosplenial Cingulate Cortex-(L). Ventral Posterior Cingulate Cortex	T(35)=8.83	0.0000	0.0000
85-31L	Precuneus-(L). Dorsal Posterior Cingulate Corte	T(35)=8.80	0.0000	0.0000
85-29R	Precuneus-(R). Retrosplenial Cingulate Cortex	T(35)=8.54	0.0000	0.0000
29L-23L	(L). Retrosplenial Cingulate Cortex- (L). Ventral Posterior Cingulate Cortex	T(35)=8.46	0.0000	0.0000
18R-19L	(R). Secondary Visual Cortex- (L) Associative Visual Cortex	T(35)=8.41	0.0000	0.0000
17R-19L	(R). Primary Visual Cortex -(L) Associative Visual Cortex	T(35)=8.36	0.0000	0.0000
18L-17R	R). Primary Visual Cortex-(R). Primary Visual Cortex	T(35)=8.93	0.0000	0.0000
18 L-19R	(L). Secondary Visual Cortex-(R). Associative Visual Cortex	T(35)=8.53	0.0000	0.0000
18L-19L	(L). Secondary Visual Cortex-(L). Associative Visual Cortex	T(35)=8.41	0.0000	0.0000
29R-30R	(R). Retrosplenial Cingulate Cortex -(R). Cingulate Cortex	T(35)=8.37	0.0000	0.0000
18L-37L	(L). Secondary Visual Cortex-(L). Fusiform gyrus	T(35)=8.21	0.0000	0.0000
17L-19R	(L). Primary Visual Cortex- (R) Associative Visual Cortex	T(35)=8.20	0.0000	0.0000
29L-85	(L). Retrosplenial Cingulate Cortex- Precuneus	T(35)=8.14	0.0000	0.0000
31R-85	(R). Dorsal Posterior Cingulate Cortex-Precuneus	T(35)=7.76	0.0000	0.0000
30L-85	(L). Cingulate Cortex- Precuneus	T(35)=7.51	0.0000	0.0000

The More Significant ROI-ROI Connections In APOE e4 Carriers Versus Non-Carrier. In this table we only included ROI-ROI connections that were more significantly connected at a .00001 two-sided FDR-p value

processing issues. Overall, these findings support the previously established theory that AD and its earlier manifestation of EMCI is a disconnection syndrome and is a result of loss of normal connectivity between neuronal systems beginning with the isolation of the hippocampal formation (Delbeuck et al. 2007). We hypothesize that this disruption of neural input and output of the hippocampus to the surrounding areas

is a contributing factor to the change in cognitive and memory function seen in EMCI.

Along with the hippocampus, previous results have shown that the PCC and medial prefrontal cortex are important hub regions in the human brain (Tomasi and Volkow 2010; Buckner et al. 2009). Hub regions exchange information with many other regions and largely influence information

Table 8 Subject group versus *APOE* group ROI

ROI	Area	Stats	Intensity	Size	*P* value
85	Precuneus	X(24)=75.62	327.83	10	0.0000
17L	(L). Primary Visual Cortex	X(24)=75.46	364.42	6	0.0000
18R	(R). Inferior Temporal Gyrus	X(24)=73.87	336.64	7	0.0000

The More Significantly Connected Regions In APOE e4 Non-Carrier Control Subjects Versus APOE e4 Carrier and EMCI subjects. In this table we only included ROI that were more significantly connected at a .00001 two-sided FDR-p value

Fig. 3 Superior, inferior, right, left, anterior view APOE e4 non-carrier controls > APOE e4 carriers and EMCI connectivity: significant ROI, and ROI-ROI connections in APOE e4 non-carrier control subjects compared to any other group. *Red* to *green*= more to less significant
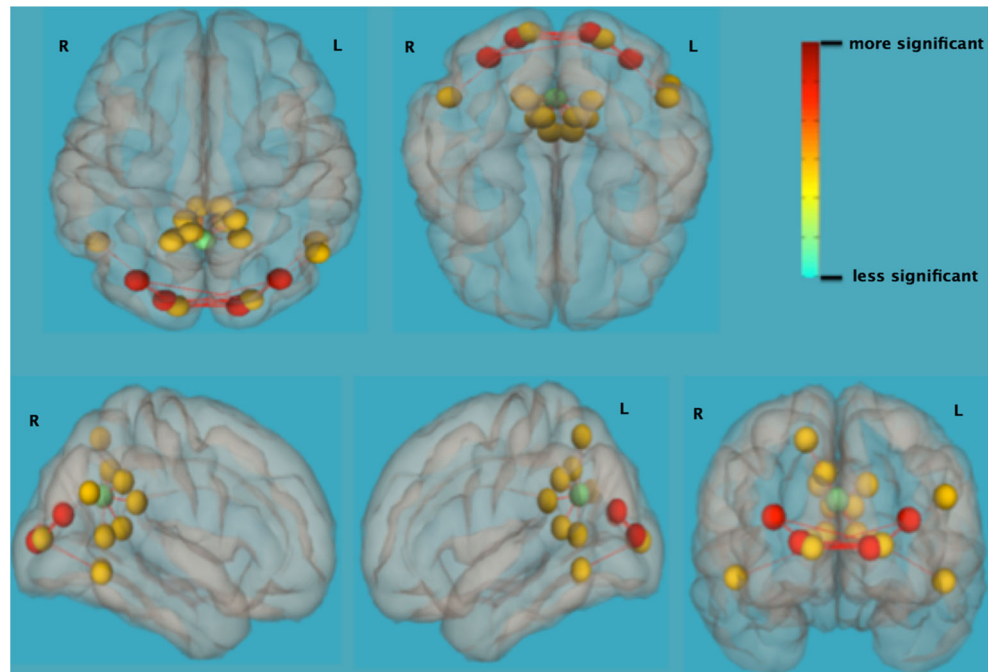
communication and functional integration between many functionally separate brain regions (Sporns 2011). Therefore, we would expect the functional connectivity abnormalities in the PCC and MPFC hub regions observed in the EMCI group to have wide-spread and significant implications. Buckner et al. (2005) hypothesized that the high use of these hub

Table 9 Subject group versus gene group connections

ROI	Area	Strength	P-unc value	p-FDR value
17L-18L	L Primary Visual Cortex- L Secondary Visual Cortex	$F(3)(33)=121.13$	0.0000	0.0000
17R-18R	R Primary Visual Cortex- R Secondary Visual Cortex	$F(3)(33)=74.50$	0.0000	0.0000
18R-18L	R &L Secondary Visual Cortex	$F(3)(33)=70.84$	0.0000	0.0000
17L-17R	L Primary Visual Cortex –			
R Primary Visual Cortex	$F(3)(33)=67.26$	0.0000	0.0000	
17L -18R	L Primary Visual Cortex- R Secondary Visual Cortex	$F(3)(33)=65.19$	0.0000	0.0000
17L-19R	L Primary Visual Cortex- R Associative Visual Cortex	$F(3)(33)=59.09$	0.0000	0.0000
18R-19R	R Secondary Visual Cortex- R Associative Visual Cortex	$F(3)(33)=50.44$	0.0000	0.0000
85-PCC	Precuneus- Posterior Cingulate Cortex	$F(3)(33)=46.63$	0.0000	0.0000
85-29R	PCC- R Retrosplenial Cingulate Cortex	$F(3)(33)=41.94$	0.0000	0.0000
85-31L	PCC-L Dorsal Posterior Cingulate Cortex	$F(3)(33)=37.46$	0.0000	0.0000
85-31R	PCC- R Dorsal Posterior Cingulate Cortex	$F(3)(33)=37.21$	0.0000	0.0000
85-23L	PCC-(L). Ventral Posterior Cingulate Cortex	$F(3)(33)=36.08$	0.0000	0.0000
85-23R	PCC- (R). Ventral Posterior Cingulate Cortex	$F(3)(33)=31.14$	0.0000	0.0000
31L-PCC	L Dorsal Posterior Cingulate Cortex-PCC	$F(3)(33)=30.81$	0.0000	0.0000
17L-19R	L Primary Visual Cortex - R Associative Visual Cortex	$F(3)(33)=29.91$	0.0000	0.0000
85-7L	PCC-(L). Somatosensory Association	$F(3)(33)=24.89$	0.0000	0.0000
18R-37R	R Secondary Visual Cortex-(R). Fusiform gyrus	$F(3)(33)=23.82$	0.0000	0.0000
85-30L	PCC-L Cingulate Cortex	$F(3)(33)=22.30$	0.0000	0.0000
17L-37L	L Primary Visual Cortex-(L). Fusiform gyrus	$F(3)(33)=21.85$	0.0000	0.0000
85-30R	PCC- R Cingulate Cortex	$F(3)(33)=19.39$	0.0000	0.0000
18R-39R	R Secondary Visual Cortex-(R). Angular gyrus	$F(3)(33)=15.66$	0.0000	0.0000

The More Significant ROI-ROI Connections In APOE e4 Non-Carrier Control Subjects Versus APOE e4 Carrier and EMCI Subjects. In this table we only included ROI-ROI connections that were more significantly connected at a .00001 two-sided FDR-p value

regions in daily life could increase the accumulation of amyloid plaques, and result in the observed functional abnormalities of EMCI and AD.

Visual networks

In EMCI subjects there was also disruption of the network connectivity in the primary, secondary and associative visual cortices (see Tables 4 and 5). The visual cortex areas are associated with the repository of long-term visual memory, and non-specific mental imagery (Miyashita 1993; Kosslyn et al. 2001). Consequently, the reduced connectivity in these non-specific regions in EMCI subjects may be a contributing factor to their memory impairment (Buckner and Wheeler 2001). Wang et al. (2006) demonstrated disrupted connectivity between the hippocampus and higher-order visual cortices in early AD, which is consistent with our findings. Buckner and Wheeler (2001) had similar findings, and proposed that the retrieval of visual information from episodic long-term memory is fulfilled by neural interactions between the medial temporal lobe structures and the posterior neocortex like the occipital sulcus. The functional disconnection between the more primary 'memory centers' in the brain these less specific memory centers like the visual cortices could be a reflection of the breakdown of hippocampal and medial temporal lobe-related cortical networks in early dementia.

DMN

It is also important to point out that a number of the areas of decrease in nodal strength in the EMCI subjects are a part of the default mode network (DMN). The DMN is a task-negative network that is most active during wakeful rest, and includes the MTL, MPFC, PCC, precuneus and the medial, lateral and inferior parietal cortex (Greicius et al. 2004). The specific function of the DMN is still unclear, but the network is thought to be related to self-referential thought, daydreaming and memory recall (Greicius et al. 2004). The documented decline of nodal strength in the DMN of EMCI subjects in our study is consistent with previous studies and suggests memory-related deficits in EMCI cognitive ability are linked to disrupted DMN function (Zhong et al. 2014; Greicius et al. 2004).

Comparison of *APOE* group network connectivity differences

We found significantly decreased RSFC in the brains of the subjects with APOE e4. This group showed decreased RSFC strength in ROIs and ROI-to-ROI connections at the .00001 FDR-p threshold level (see Tables 5 and 6). The APOE allele e4 is the best-known genetic risk factor for sporadic AD (Mahley et al. 2006). We found that this group to have unique

RSFC, which could be the result of a unique early dementia pathology.

Prefrontal areas

As discussed above, the notable difference between APOE allele e4 carrier decrease in RSFC and the EMCI group decrease in RSFC was in the prefrontal lobe areas. Both subject groups are at risk for developing AD and showed overall similarities in RSFC decrease, but the APOE allele e4 carrier group did not show disrupted network function in frontal lobe structures at the same FDR-p threshold level (see Fig. 2). The prefrontal cortex is known to atrophy naturally with age, and the prefrontal cortex RSFC weakness observed in the EMCI group could be an effect of natural age-related morphometry instead of APOE e4 (Euston et al. 2002a, b). Our findings suggest that prefrontal lobe connectivity weakness could be a symptom that separates EMCI individuals into those with more natural aging-related memory loss versus APOE e4-related memory loss. EMCI is the earliest form of dementia and not all EMCI diagnosed patients develop AD (Jessen et al. 2014). Patients with EMCI who have more disrupted frontal lobe RS-FC could have a unique pathology, with a different risk probability of developing AD.

Cingulate cortex and associated areas

Similar to the EMCI group, the group containing the APOE allele 4 had decreased RSFC in the cingulate cortices and surrounding hippocampal areas (see Tables 6 and 7). Filippini et al. (2009), found those with APOE e4 to have altered RSFC between hippocampal, medial prefrontal, and retrosplenial regions of the brain in the DMN in carriers relative to non-carriers, consistent with our findings. Since both the EMCI and APOE e4-containing groups were shown to have similar affected brain areas, the decrease in RSFC in the brains of those with APOE e4 could interfere with their ability to cope with increasing levels of AD pathology in the same areas. EMCI patients without APOE allele e4 appear to show similar changes in brain function with age, but have a reduced risk of developing AD (Sheline et al. 2010). To further strengthen this argument, we found that the regions of decreased RSFC in healthy controls with APOE e4 overlapped with the regions of decreased RSFC in the EMCI group.

Visual areas

Similar to the EMCI subject group, the group containing APOE e4 had decreased RSFC in the primary, secondary and associative visual cortices (see Tables 6 and 7). As discussed above, the visual cortex areas are associated with mental imagery and memory recall (Buckner and Wheeler

2001). Trachtenberg et al. (2011) found that APOE allele e4 carriers had decreased connectivity in the primary visual cortex similar to our results. The APOE e4 carrier groups' weakness in RSFC between both the more primary 'memory center' ROI in the brain like the cingulate cortex, precuneus and less specific memory center ROI like the visual cortices could be a reflection of how complex APOE e4 pathology is and the role of this gene on brain development. As theorized above, the decrease in RS-FC in the brains of APOE e4-carriers could interfere with the ability of this group to cope with increasing levels of AD pathology in the same areas.

The results observed here, especially in parallel to the EMCI group findings, can provide insight into the relationship between APOE e4, brain function and AD risk. The similar but not identical pattern of disconnectivity and weakness in functional connectivity between the EMCI and APOE e4-carrier groups suggests that the pathology is similar but EMCI pathology is more multidimensional. Highlighting the differences between the EMCI and APOE e4 linked pathologies can illustrate how EMCI phenotypes differ, and how APOE e4 could predispose people to the disease.

Comparison of subject groups' versus *APOE* groups

Groups' network connectivity differences

We found significant differences in RSFC by comparing the two subject groups to the *APOE* groups. Subjects who were controls and APOE e4 non-carriers, had stronger ROI connectivity in 3 ROI (see Table 8, Fig. 3). The same group had 21 significantly stronger ROI-ROI specific connections (see Table 9). The subjects who either had APOE e4 and/or were EMCI had No ROI or ROI-ROI connection strengths that were significant at the .00001 significant threshold. This multi-group analysis reaffirmed the previous findings from between-group analyses that RSFC dysfunction occurs most strongly in EMCI subjects, and in those with the APOE allele e4. This analysis further shows that within the EMCI group the greatest dysfunction in RSFC is happening in those with the ApoE4 genotype and most strongly affecting the precuneus, primary visual cortex and inferior temporal gyrus (See Table 8). As discussed above, these ROIs are all important areas for memory and cognition. The precuneus is involved with episodic memory, while the inferior temporal gyrus is associated with semantic memory and the primary visual cortex functions in working memory.

These group comparison findings show that although the EMCI APOE e4 carrier group showed only a few ROI with total RSFC strength decrease, they showed dysfunction in connectivity between 21 ROIs (see Tables 7 and 8). This finding highlights that within the EMCI APOE e4-carrier population the greatest RSFC disturbance is happening in the individual connections between ROIs with significant memory

and cognitive function. This could be an unique dementia pathology specific to EMCI phenotypes with APOE e4. This compares to our findings on RSFC in the EMCI subject group as a whole with a variety of APOE alleles, which had a greater variety of areas of RSFC dysfunction including the prefrontal lobe and other MTL structures but without as much dysfunction in individual connections between ROI. There is a similar but not identical pattern of disconnectivity and weakness in RSFC between the APOE e4 carrier group as a whole and the APOE e4 carrier group only containing EMCI subjects. This suggests that APOE e4 affects both normal aging and EMCI subjects similarly. The distinct pattern of RSFC dysfunction in the EMCI APOE e4 carrier group highlights how APOE e4 pathology could be interacting with other EMCI factors to create a specific EMCI phenotype that predominantly has weak connectivity between a number of important ROIs including the visual cortices, PCC, retrosplenial cingulate cortices, cingulate cortices, precuneus and fusiform gyrus (see Table 8).

Several studies have used fMRI to study the effects of APOE e4 on brain function, but most have only studied normal populations and only in specific RSN or brain areas. This final multi-group analysis shows a novel finding by investigating the effect of APOE e4 on a control, EMCI and mixed subjects pool. The results from this analysis are particularly interesting because we did not restrict the ROI analysis, and the results show whole-brain analysis findings. Also, these results have very high statistical significance because they were set at a .00001 FDR-p value threshold as to only obtain the greatest changes in RSFC.

Conclusions

Our results show that there are distinct differences in RSFC between EMCI and normal aging subjects, between APOE e4 carriers and non-carriers, and between EMCI subjects who are APOE e4 carriers and non-carriers. As expected from previous research, RSFC network properties were disrupted in EMCI. Our findings highlighted the EMCI RSFC decrease in a variety of important functionally linked ROI: visual cortices, temporal gyrus, the precuneus, the retrosplenial cingulate cortices, the PCC, MPFC and the anterior cingulate cortices. Our findings also show the strong overlap in decreased RSFC between the EMCI group and the APOE e4 carrier group, supporting previous research on APOE e4 playing a strong role in developing EMCI. We found that only the EMCI group had a decrease in RSFC of the prefrontal cortex areas, which suggests that EMCI pathology is more multidimensional than the APOE e4 genetic AD predisposition alone. Not surprisingly, the control APOE e4 non-carrier group showed the least RS-FC dysfunction and most significant difference in comparison to the other groups in ROI

strength and connectivity. Interestingly, this Control APOE e4 non-carrier group showed more significant RSFC most predominantly in the individual connections between ROI, versus in the strength of ROIs. Therefore, EMCI and APOE e4 carrier populations may have a unique dementia pathology that mostly affects connectivity between specific areas with memory and cognition functions.

Previous research has used fMRI to study the effects of APOE e4 on brain function, but none have used matched EMCI and control subjects to look at the APOE e4 effect on each group and the subjects as a whole. Also, few groups have used whole-brain ROI-to-ROI analysis to investigate the broad impact of both EMCI and on the RS-FC of the brain. By using this type of analysis we provided evidence that EMCI is a disease with multiple factors, and that APOE e4 has a similar and most likely contributing pathology. We also show that the APOE e4 affect on RS-FC is similar across healthy controls and EMCI subjects. This opens up the investigation of what other factors interact with APOE e4 to cause EMCI.

Limitations

When considering the size and generalizability of the study in comparison to relation to prior studies using rs-fMRI to explore stages of AD, this study had an average sample size. The 55 prior studies published in the past 2 years on this topic used a median total sample of 37 subjects (Delbeuck et al. 2007). Our sample was composed of N 36 subjects, which although not large in absolute terms, is comparable to previous literature. Out of N 36 subjects we subdivided our groups into 18 and 18 for the first two Group and *APOE* analyses, and 12 and 24 for the third Control APOE e4 non-carrier versus EMCI and APOE e4 carrier analysis (see Tables 1 and 2). Therefore, our results seem to be generalizable. We would propose future research to use larger sample sizes, which would be able to breakdown the APOE carrier types more specifically than with or without APOE allele e4 groups. This more specific APOE analysis could reveal more detailed information on how each APOE carrier type affects EMCI and its unique RSFC.

References

Behzadi, Y., Restom, K., Liau, J., & Liu, T. T. (2007). A component based noise correction method (CompCor) for BOLD and perfusion based fMRI. *NeuroImage 37*, 90–101.

Buckner, R. (2004). Memory and executive function in aging and AD: multiple factors that cause decline and reserve factors that compensate. *Neuron, 44*, 195–208.

Buckner, R. L., & Wheeler, M. E. (2001). The cognitive neuroscience of remembering. *Nature Reviews Neuroscience, 2*, 624–634.

Buckner, R., Snyder, A., Shannon, B., LaRossa, G., Sachs, R., Fotenos, A., Klunk, W., & Mathis, C. (2005). Molecular, structural, and functional characterization of Alzheimer's disease: evidence for a relationship between default activity, amyloid, and memory. *Journal of Neuroscience, 23*(34), 7709–7717.

Buckner, R. L., Sepulcre, J., Talukdar, T., Krienen, F. M., Liu, H., Hedden, T., Andrews-Hanna, J. R., Sperling, R. A., & Johnson, K. A. (2009). Cortical hubs revealed by intrinsic functional connectivity: mapping, assessment of stability, and relation to Alzheimer's disease. *Journal of Neuroscience 29*, 1860–1873.

DeLaPaz, R. L. (1994). Echo-planar imaging. *Radiographics, 14*, 1045–1058.

Delbeuck, X., Collette, F., & Van der Linden, M. (2007). Is Alzheimer's disease a disconnection syndrome? Evidence from a crossmodal audio-visual illusory experiment. *Neuropsychologia, 45*(14), 3315–3323.

Euston, D. R., Gruber, A. J., & McNaughton, B. L. (2002). The role of medial prefrontal cortex in memory and decision making. *Neuron, 76*(6), 1057–1070.

Filippini, N., MacIntosh, B., Hough, M., Goodwin, G., Frisoni, G., Smith, S., et al. (2009). Distinct patterns of brain activity in young carriers of the APOE-varepsilon4 allele. *Proceedings of the National Academy of Sciences of the United States of America, 106*, 7209–7214.

Fox, M. D., Snyder, A. Z., Vincent, J. L., Corbetta, M., Van Essen, D. C., & Raichle, M. E. (2005). The human brain is intrinsically organized into dynamic, anticorrelated functional networks. *Proceedings of the National Academy of Sciences of the United States of America, 102*, 9673–9678.

FreeSurfer Welcome. (2014). Retrieved October 1, 2014, from http://freesurfer.net/fswiki.

Greicius, M., Srivastava, G., Reiss, A., & Menon, V. (2004). Default-mode network distinguishes Alzheimer's disease from healthy aging: evidence from functional MRI. *Proceedings of the National Academy of Sciences of the United States of America, 101*(13), 4637–4642.

Jessen, F., Wolfsgruber, S., Wiese, B., Bickel, H., Mosch, E., Kaduszkiewicz, H., Pentzek, M., Riedel-Heller, M. G., Luck, T., Fuchs, A., Weyerer, S., Werle, J., Van den Bussche, H., Schere, M., Maier, W., & Wagner, M. (2014). AD dementia risk in late MCI, in early MCI, and in subjective memory impairment. *Alzheimer's & Dementia, 10*(1), 76–83.

Kobayashi, Y., & Amaral, D. G. (2003). Macaque monkey retro-splenial cortex: cortical afferents. *Journal of Comparative Neurology, 466*, 48–79.

Kosslyn, S. M., Ganis, G., & Thompson, W. L. (2001). Neural foundations of imagery. *Nature Reviews Neuroscience, 2*, 635–642.

Machulda, M. M., Jones, D. T., Vemuri, P., McDade, E., & Avula, R. (2011). Effect of APOE epsilon4 status on intrinsic network connectivity in cognitively normal elderly subjects. *Archives of Neurology, 68*, 1131–1136.

Mahley, R. W., Weisgraber, K. H., & Huang, Y. (2006). Apolipoprotein E4: a causative factor and therapeutic target in neuropathology, including Alzheimer's disease. *Proceedings of the National Academy of Sciences of the United States of America, 103*(15), 5644–5645.

Miyashita, Y. (1993). Inferior temporal cortex: where visual perception meets memory. *Annual Review of Neuroscience, 16*, 245–263.

Mueller, S. G., Weiner, M. W., Thal, L. J., Petersen, R. C., Jack, C. R., Jagust, W., Trojanowski, J. Q., Toga, A. W., & Becket, L. (2005). Ways toward an early diagnosis in Alzheimer's disease: the Alzheimer's disease neuroimaging initiative (ADNI). *Alzheimer's Dementia, 1*, 55–66.

Petersen, R., & Weiner, M. (2014). Alzheimer's Disease Neuroimaging Initiative 2 (ADNI2) Protocol. Retrieved from www.adni-info.org/Scientists/ADNIStudyProcedure.

Petersen, R. C., Smith, G. E., Waring, S. C., Ivnik, R. J., Tangalos, E. G., & Kokmen, E. (1999). Mild cognitive impairment: clinical characterization and outcome. *Archives of Neurology, 56*, 303–308.

Roid, G., Prifitera, A., & Ledbetter, M. (2007). Confirmation analysis of the factor structure of the wechsler memory scale-revised. *Clinical Neuropsychologist, 2*(2), 116–120.

RStudio. (2014). RStudio: Integrated development environment for R (Version 0.96.122) [Computer software]. Boston, MA. Retrieved October 20, 2014. Available from http://www.rstudio.org/

Sanz-Arigita, E. J., Schoonheim, M. M., Damoiseaux, J. S., Rombouts, S. A., & Maris, E. (2010). Loss of 'small-world' networks in Alzheimer's disease: graph analysis of FMRI resting-state functional connectivity. *PloS One, 5*, 13788.

Sheline, Y. I., Morris, J. C., Snyder, A. Z., Price, J. L., Yan, Z., & D'Angelo, G. (2010). APOE4 allele disrupts resting state fMRI connectivity in the absence of amyloid plaques or decreased CSF Aβ42. *Journal of Neuroscience, 30*(50), 17035–17040.

Sporns, O. (2011). The human connectome: a complex network. *Annals of the New York Academy of Sciences, 1224*, 109–125.

Supekar, K., Menon, V., Rubin, D., Musen, M., & Greicius, M. D. (2008). Network analysis of intrinsic functional brain connectivity in Alzheimer's disease. *PLoS Computational Biology, 4*(6), e1000100. doi:10.1371/journal.pcbi.1000100.

Tomasi, D., & Volkow, N. D. (2010). Functional connectivity density mapping. *Proceedings of the National Academy of Sciences of the United States of America, 107*, 9885–9890.

Trachtenberg, A. J., Filippini, N., Cheeseman, J., Duff, E. P., Neville, M. J., Ebmeier, K. P., Karpe, F., & Mackay, C. E. (2011). The effects of APOE on brain activity do not simply reflect the risk of Alzheimer's disease. *Neurobiol. Aging*. doi:10.1016/j.neurobiolaging.2010.11.011.

Wang, L., Zang, Y., He, Y., Liang, M., Zhang, X., Tian, L., Wu, T., Jiang, T., & Li, K. (2006). Changes in hippocampal connectivity in the early stages of Alzheimer's disease: evidence from resting state fMRI. *NeuroImage, 31*, 496–504.

Wang, K., Liang, M., Wang, L., Tian, L., Zhang, X., Li, K., & Jiang, T. (2007). Altered functional connectivity in early Alzheimer's disease: a resting-state fMRI study. *Human Brain Mapping, 28*, 967–978.

Whitfield-Gabrieli, S., & Nieto-Castanon, A. (2012). Conn: A functional connectivity toolbox for correlated and anticorrelated brain networks. *Brain Connectivity, 2*(3), 125–141. doi:10.1089/brain.2012.0073.

Zhong, Y., Huang, L., Cai, S., Zhang, Y., von Deneen, K., & Ren, A. (2014). Altered effective connectivity patterns of the default mode network in Alzheimer's disease: an fMRI study. *Neuroscience Letters, 578*, 171–175.